

Exosomes Derived from Hypoxic Oral Squamous Cell Carcinoma Cells Deliver miR-21 to Normoxic Cells to Elicit a Prometastatic Phenotype

Ling Li^{1,2}, Chao Li¹, Shaoxin Wang¹, Zhaohui Wang¹, Jian Jiang³, Wei Wang¹, Xiaoxia Li¹, Jin Chen¹, Kun Liu^{1,2}, Chunhua Li¹, and Guiquan Zhu¹

Abstract

Hypoxia is a common feature of solid tumors and is associated with aggressiveness and poor patient outcomes. Exosomes, initially considered to be cellular "garbage dumpsters," are now implicated in mediating interactions with the cellular environment. However, the mechanisms underlying the association between exosomes and hypoxia during cancer progression remain poorly understood. In this study, we found that exosomes derived from hypoxic oral squamous cell carcinoma (OSCC) cells increased the migration and invasion of OSCC cells in a HIF-1 α and HIF-2 α -dependent manner. Given that exosomes have been shown to transport miRNAs to alter cellular functions, we performed miRNA sequencing of normoxic and hypoxic OSCC-derived exosomes. Of the 108 miRNAs that were differentially expressed, miR-21 stood out as one of the most significantly upregulated miRNAs under hypoxic conditions. miR-21 deple-

tion in hypoxic OSCC cells led to decreased miR-21 levels in exosomes and significantly reduced cell migration and invasion. Conversely, restoration of miR-21 expression in HIF-1 α and HIF-2 α -depleted exosomes rescued OSCC cell migration and invasion. Moreover, exosomal miR-21 markedly enhanced snail and vimentin expression, while significantly decreasing E-cadherin levels in OSCC cells, *in vitro* and *in vivo*. Finally, circulating exosomal miR-21 levels were closely associated with HIF-1 α /HIF-2 α expression, T stage, and lymph node metastasis in patients with OSCC. In conclusion, our findings suggest that the hypoxic microenvironment may stimulate tumor cells to generate miR-21-rich exosomes that are delivered to normoxic cells to promote prometastatic behaviors and prompt further investigation into the therapeutic value of exosome inhibition for cancer treatment. *Cancer Res*; 76(7); 1770–80. ©2016 AACR.

Introduction

Oral squamous cell carcinoma (OSCC) accounts for 24% of all head and neck cancers, with an estimated incidence of 300,000 cases per year worldwide (1). More than 50% of OSCC patients exhibit lymph node metastasis, which is one of the most common adverse prognostic factors in OSCC patients (2, 3). Five-year survival rates for patients with localized OSCC are greater than 80% but drop to 40% when the lymph nodes are involved, and to 20% for patients with distant metastasis (4). It has been increasingly recognized that hypoxia, which is commonly defined as a condition in tissues where the oxygen pressure is less than 5 to 10 mm Hg, is a powerful driving force for cancer metastasis (5, 6).

A highly proliferating mass of tumor cells develops more quickly than the vasculature, and tumor cells thus encounter an

avasascular microenvironment deficient in oxygen, that is, hypoxia (7). Such hypoxic zones have been postulated to act as an incubator for a malignant evolution, where more aggressive cancer cells are selected. Recent studies show that each step of the metastatic process, from the initial epithelial–mesenchymal transition (EMT) to the ultimate organotropic colonization, can potentially be regulated by hypoxia, suggesting a master regulatory role for hypoxia in metastasis (5). The major mechanism mediating adaptive responses to hypoxia are the stabilization and activation of the hypoxia-inducible factors (HIF), especially HIF-1 α and HIF-2 α . HIF-1 α and HIF-2 α activate a set of genes that facilitate tumor growth, angiogenesis, and metastasis (8, 9). Although HIF-1 α and HIF-2 α have striking similarities in structure, function, and regulation, many lines of evidence suggest that these two HIF- α proteins play distinct and functionally overlapping roles in tumor progression (10).

Exosomes are small, 30 to 100-nm membrane vesicles formed by the inward budding of late endosomes that are released into the extracellular environment upon fusion with the plasma membrane (11–13). Many cell types can produce exosomes, including dendritic cells, B cells, T cells, mast cells, epithelial cells, and tumor cells (14). Although initially considered to be products of a pathway used to release unwanted material from cells, exosomes are now believed to perform a variety of extracellular functions that involve interactions with the cellular microenvironment, such as morphogen signaling, immunologic mediation, cell recruitment, and horizontal transfer of genetic material (15, 16). Exosomes contain a wide range of functional proteins, mRNAs and miRNAs (17–19) that allow these structures to

¹Department of Head and Neck Surgery, Sichuan Cancer Hospital & Institute, Sichuan, P.R. China. ²Department of Stomatology, Sichuan Cancer Hospital & Institute, Sichuan, P.R. China. ³State Key Laboratory of Oral Diseases, West China Hospital of Stomatology, Sichuan University, Sichuan, P.R. China.

Note: Supplementary data for this article are available at Cancer Research Online (<http://cancerres.aacrjournals.org/>).

Corresponding Author: Guiquan Zhu, Department of Head and Neck Surgery, Sichuan Cancer Hospital & Institute, No. 55, Section 4, Renmin South Road, Chengdu, Sichuan 610041, P.R. China. Phone: 8628-8542-0166; Fax: 8628-8542-0251; E-mail: headnecksurg@foxmail.com

doi: 10.1158/0008-5472.CAN-15-1625

©2016 American Association for Cancer Research.

operate as signaling platforms for short-range or long-range delivery of information to other cells (20). Tumor cells secrete large amounts of exosomes that promote tumor progression through communication between the tumor and surrounding stromal tissue, activation of proliferative and angiogenic pathways, and initiation of premetastatic sites (21–25). Therefore, exosomes are an important component of the tumor microenvironment and are currently considered to be one of the main contributors to tumor progression and metastasis (15).

It has been shown that hypoxia may promote the release of exosomes by breast cancer cells in a HIF-1 α -dependent manner (21). Kucharzewska and colleagues (26) showed that glioblastoma multiforme cell-derived hypoxic exosomes are potent inducers of angiogenesis through the phenotypic modulation of endothelial cells. Park and colleagues (27) showed that hypoxia could induce tumor cells secretion of proteins with the potential to modulate their microenvironment and facilitate angiogenesis and metastasis. More than 50% of the secreted proteins were found in exosomes (27). More recently, Tadokoro and colleagues (28) demonstrated that hypoxia altered the miRNA profiles of tumor-derived exosomes, which affected angiogenic activity in endothelial cells. These results suggest that tumor-derived exosomes may, at least in part, mediate the hypoxic evolution of the cancer microenvironment through transported miRNAs. We therefore hypothesized that miRNAs can be transported from hypoxic cancer cells to normoxic cells through exosomes, by which the hypoxic microenvironment can modulate the bioactivity of normoxic cells.

Materials and Methods

Human and animal studies have been approved by the Institutional Ethics Committee of Sichuan Cancer Hospital and West-China Hospital of Stomatology (Sichuan, P.R. China). Detailed protocols are listed in the Supplementary Materials and Methods.

Patients

One hundred and eight patients with newly diagnosed OSCC were enrolled in this study at Sichuan Cancer Hospital and West-China Hospital of Stomatology from May 2011 to September 2014. The principal clinical and pathologic characteristics of the patient cohort are summarized in Table 1. In addition, healthy blood samples were obtained from 108 volunteers without any malignancy.

shRNA cloning and lentiviral packaging

The Lenti-X shRNA expression system (Clontech) was used for the shRNA-mediated inhibition of HIF-1 α and HIF-2 α expression, and the knocking down efficiency of HIF-1 α and HIF-2 α lentiviral shRNAs has been demonstrated in our previous study (29). To knock down miR-21 expression, oligonucleotides against miR-21 were annealed and cloned into the lentiviral vector pLenti-U6-pgkpuro as described previously (30).

Cell culture and hypoxia treatment

Two human OSCC cell lines SCC-9 and CAL-27 were obtained from the State Key Laboratory of Oral Disease, Sichuan University (Sichuan, P.R. China). The cell lines were last authenticated by short tandem repeat DNA fingerprinting on April 6, 2015. Cells were cultured in RPMI1640 medium (Gibco) in a humidified 5%

Table 1. Clinical-pathologic characteristic of 108 patients with OSCC, and association between circulating exosomal miR-21 level and these variables (using median miR-21 level as the cutoff)

Clinical-pathological variables	NO. of patients	Exosomal miR-21		P
		Low	High	
Overall	108	54	54	
Gender				
Female	45	24	21	0.562
Male	63	30	33	
Age				
≤ 60	41	23	18	0.326
> 60	67	31	36	
T Stage				
T1/T2	39	26	13	0.009
T3/T4	69	28	41	
N Stage				
N0	33	22	11	0.021
N1/N2/N3	75	32	43	
Histologic differentiation				
Well	32	18	14	0.092
Moderate	49	27	22	
Poorly	27	9	18	
Recurrence				
No	29	16	13	0.519
Yes	79	38	41	
HIF-1 α				
Negative	51	34	17	0.001
Positive	57	20	37	
HIF-2 α				
Negative	43	29	14	0.003
Positive	65	25	40	

NOTE: Bold indicates significance.

CO₂ atmosphere. The cells were cultured under 20% O₂ (normoxic) or 1% O₂ (hypoxic) conditions, balanced with N₂ in a 3-gas incubator (Binder).

Exosome isolation, labeling, and RNA extraction

A total of 250 μ L of serum or 10 mL of tissue culture media was mixed with ExoQuick exosome precipitation solution and exosome isolation was performed according to the manufacturer's instructions (SBI System Biosciences). Purified exosomes were labeled with the green fluorescent linker PKH67 (Sigma) as described previously (31).

Electron microscopy

Exosomes to be examined by scanning electron microscopy (SEM) were isolated and loaded on to a carbon-coated electron microscopy grid as described previously (32). The samples were fixed with 2% glutaraldehyde and 2% paraformaldehyde in 0.1 mol/L sodium cacodylate buffer at pH 7.3 for 3 hours at room temperature. Samples were critical-point dried, mounted on specimen stubs, sputter-coated, and visualized using a Hitachi S3400 scanning electron microscope.

miRNA library construction and sequencing

Total RNAs from exosomes was used for miRNA library preparation and sequencing. Library preparation and sequencing was performed at RiboBio. Briefly, total RNA samples were fractionated on a 15% Tris-borate-EDTA (TBE) polyacrylamide gel (Invitrogen) and small RNAs ranging between 18 and 30 nucleotides (nt) were used for library preparation. Small RNAs were reverse transcribed and amplified by PCR. The PCR products were sequenced using the Illumina HiSeq 2500 platform.

qRT-PCR

Quantification of miRNA expression was performed using the NCode EXPRESS SYBR GreenER miRNA qRT-PCR Kit (Invitrogen) on an ABI PRISM 7300 Sequence Detection System (Applied Biosystems). cel-miR-39 was used to normalize for technical variation between the samples as described previously (33).

Immunofluorescence and immunohistochemistry

Slides were incubated at 37°C with mouse anti-HIF-1 α (1:200, Novus), mouse anti-HIF-2 α (1:100, Abcam), rabbit anti-E-Cadherin (1:100, Abcam), and mouse anti-vimentin (1:100, Abcam) for 2 hours. For IHC, slices were then incubated with biotinylated goat anti-mouse IgG for 1 hour, and streptavidin-peroxidase for 30 minutes. For immunofluorescence (IF) double staining, slides were incubated for 1 hour with Alexa Fluor 488 goat anti-mouse IgG (1:500, Invitrogen) and Alexa Fluor 594 goat anti-rabbit IgG (1:500, Invitrogen).

Western blot analysis

Thirty micrograms of protein was separated on an 8% SDS-PAGE gel and transferred to polyvinylidenedifluoride membranes (Millipore). Membranes were blocked and then incubated for 2 hours with either mouse anti-CD81 (1:1,000, Santa Cruz Biotechnology), mouse anti-CD63 (1:1,000, Santa Cruz Biotechnology), rabbit anti-E-cadherin (1:1,000, Abcam), mouse anti-vimentin (1:1,000, Abcam), rabbit anti-snail (1:1,000, Abcam), rabbit anti-PTEN (1:1,000, Cell Signaling Technology), rabbit anti-Pdcd4 (1:1,000, Thermo Fisher Scientific), or rabbit anti-tubulin (1:1,000, Novus). Horseradish peroxidase-conjugated anti-mouse or anti-rabbit IgG was used as a secondary antibody (diluted 1:5,000 in TBST). Bands were scanned using a densitometer (GS-700; Bio-Rad Laboratories), and quantification was performed using Quantity One 4.4.0 software.

Xenografts

The Nude mice (females, 6 weeks of age) were obtained from the Laboratory Animal Center of Sichuan University (Chengdu, Sichuan, P.R. China). Cells were injected subcutaneously (5×10^6 cells/200 μ L PBS/mouse) into the back of nude mice. The tumor size was monitored weekly by measuring diameters using vernier calipers, and calculated as $\pi l^2/6$, where l = the long side and s = the short side, as described previously (34).

Scratch assay

The scratch assay was performed to measure cell migration *in vitro* as described previously (35). Briefly, cells were reseeded onto 60-mm dishes to create a confluent monolayer. The cell monolayer was scraped in a straight line to create a "scratch" with a p200 pipette tip and then incubated with tumor-derived exosomes (10 μ g/mL). The first image of the scratch was acquired, and cells were cultured in the incubator at 37°C for 24 hours prior to acquisition of the second image. The percent wound closure (%) = migrated cell surface area/total surface area \times 100.

Invasion assay

A cell invasion assay was conducted with a BioCoat Matrigel Invasion Chambers (Swedesboro) according to the manufacturer's instructions. Briefly, cells were seeded into the extracellular matrix layer. Exosomes (10 μ g/mL) were added to the bottom chambers as chemoattractant. Invaded cells that had migrated to

the bottom of the insert membrane were fixed and stained with 0.4% crystal violet.

Chromatin immunoprecipitation assay

Chromatin immunoprecipitation (ChIP) assays were performed using a ChIP Assay Kit (Abcam) according to the manufacturer's instructions. Briefly, cells were fixed, lysed, and sonicated to obtain DNA fragments in arranging in size from 200 to 1,000 bp. Chromatin was then precipitated with nonspecific IgG antibodies (Sigma), ChIP-grade mouse anti-HIF-1 α (Abcam), or ChIP-grade rabbit anti-HIF-2 α (Abcam). DNA was extracted and PCR was performed with primers for a miR-21 promoter fragment containing a HIF response element (HRE; ref. 36). Primers that amplify a region in the promoter of miR-130b were used as a negative control (37).

Statistical analysis

The comparisons of means among groups were analyzed by one-way ANOVA, and the Dunn Multiple Comparison Test was further used to determine significant differences between groups. The association between circulating miR-21 levels and patients' clinical-pathologic parameters was compared using Pearson χ^2 test. All statistical analyses were performed using the SPSS package (version 13.0). A value of $P < 0.05$ was considered statistically significant.

Results

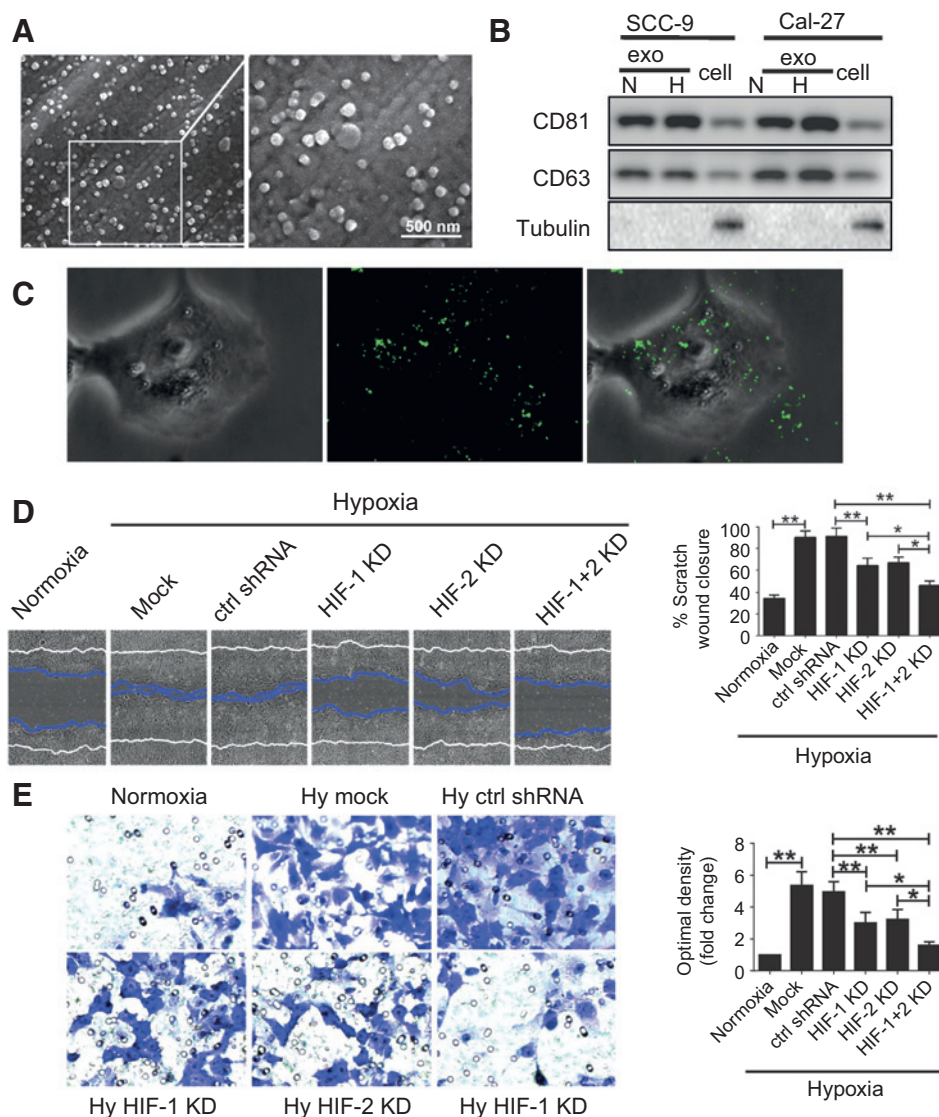
Hypoxic tumor-derived exosomes induce normoxic cell migration and invasion

Tumor-derived exosomes were initially purified from the supernatant of OSCC cells cultured under normoxic and hypoxic conditions. The purified exosomes were examined by SEM, which showed typical rounded particles ranging from 50 to 200 nm in diameter (Fig. 1A). We further confirmed the presence of the known exosome markers CD63 and CD81 by Western blot analysis (Fig. 1B). To evaluate the role of hypoxia on exosome release, we quantified the production of exosomes by immunoblotting for CD63 as described previously (21). We found that hypoxia induced the release of exosomes by both Cal-27 and SCC-9 cell lines as determined by CD63 immunoblotting (Supplementary Fig. S1).

Once secreted, exosomes deliver biologic information by internalization by neighboring or distant cells. In solid tumors, oxygen levels in hypoxic regions are less than 1%. We sought to investigate whether exosomes derived from hypoxic tumor cells could affect normoxic tumor cells. OSCC cells were cultured under 20% O₂, and treated with exosomes derived from cells cultured under conditions of 1% O₂ or 20% O₂. Tumor-derived exosomes were labeled with fluorescent PKH67. The PKH67-labeled exosomes were internalized by OSCC cells during 2-hour incubation as measured by fluorescence microscopy (Fig. 1C). We next studied the effects of hypoxic tumor-derived exosomes on the migration and invasion of normoxic OSCC cells. Wound healing assays showed that hypoxic tumor-derived exosomes significantly increased the migration (Fig. 1D) of OSCC cells compared with normoxic tumor-derived exosomes. In accordance with the migration results, cell invasion was significantly increased by hypoxic tumor-derived exosomes compared with normoxic tumor-derived exosomes (Fig. 1E). Moreover, hypoxic exosomes derived from HIF-1 α and HIF-2 α knockdown (KD) cells failed to increase cell migration and invasion. In addition, simultaneous knockdown of HIF-1 α and HIF-2 α further decreased migration and invasion

Figure 1.

Hypoxic tumor-derived exosomes induced migration and invasion of normoxic cells. **A**, representative electron micrograph of exosomes isolated from OSCC-conditioned medium revealing the typical morphology and size (50–200 nm). Scale bar, 500 nm. **B**, Western blot analysis showing the presence of CD63 and CD81 and the absence of tubulin in exosomes (exo) derived from the conditioned medium of SCC-9 and Cal-27 cells. **C**, representative confocal microscopy image showing the internalization of PKH67-labeled exosomes (green) by OSCC cells. **D**, analysis of tumor cell migration by *in vitro* scratch assay. Left, OSCC cells were treated with exosomes derived from conditioned medium as indicated. Images were acquired at 0 (white line) and 24 hours (blue line). Right, quantitative analysis of scratch wound closure. Data represent at least three experiments performed in triplicate. *, $P < 0.01$; **, $P < 0.001$. **E**, the invasiveness of exosome-treated OSCC cells was assessed using an invasion assay. Left, cells that migrated to the bottom surface were stained with crystal violet and observed by light microscopy (magnification, $\times 200$). Right, quantitative analysis of crystal violet optical density. Data represent at least three experiments performed in triplicate. *, $P < 0.01$; **, $P < 0.001$.



compared with knockdown of either alone (Fig. 1D and E). These results suggest that exosomes may be remodeled to promote tumor migration and invasion under hypoxia, and that both HIF-1 α and HIF-2 α play important roles in the remodeling of hypoxic exosomes.

miRNA expression profile of hypoxic tumor-derived exosomes

Exosomes have been demonstrated to contain both mRNAs and miRNAs, which can be delivered to other cells and affect cellular function (18). The miRNA expression profiles vary by cell type and conditions. We sought to investigate the miRNA expression profiles of exosomes derived from normoxic and hypoxic OSCC cells using Illumina HiSeq 2500 high-throughput sequencing (miRNA-seq). The OSCC cell line Cal-27 was cultured under 20% O₂ and 1% O₂. After 24 hours of treatment, exosomes from the supernatant were isolated and total RNA was prepared for miRNA-seq analysis.

Initially, a total of 2,597,268 reads were produced. After trimming low-quality reads, contaminants, adaptors, and reads smaller than 17 nt, the remaining reads were mapped to noncoding (nc)

RNA databases. Supplementary Table S1 shows the reads identified for categories of small RNA (miRNA, rRNA, tRNA, snRNA, snoRNA, piRNA, and Y_RNA) and unannotated RNAs (others). The percentage of miRNAs in the total RNA isolated from normoxic and hypoxic exosomes corresponded to 11.85% and 37.63%, respectively. There was a statistically significant ($P = 0.0057$) difference between the normoxic and hypoxic conditions (Fig. 2A).

To identify the conserved miRNAs, all ncRNA reads from normoxic and hypoxic exosome libraries were compared with the known human miRNAs in miRBase v20. To focus on the highly represented miRNAs, sequences less than 10 reads were removed. Finally, 223 and 288 types of known miRNAs in normoxic and hypoxic exosomes, respectively, were identified (Supplementary Table S2). In addition, 214 miRNAs were simultaneously identified in both groups. The number of overlapping and unique miRNAs between normoxic and hypoxic exosomes is shown in Fig. 2B. Raw sequencing data has been submitted to NCBI sequence read archive (SRA, accession number: PRJNA309559).

We next compared the expression level of miRNAs in normoxic and hypoxic exosomes. Using a 2-fold change and $P < 0.05$ as the

Downloaded from <http://aacrjournals.org/cancerres/article-pdf/76/7/1770/2747093/1770.pdf> by guest on 23 May 2025

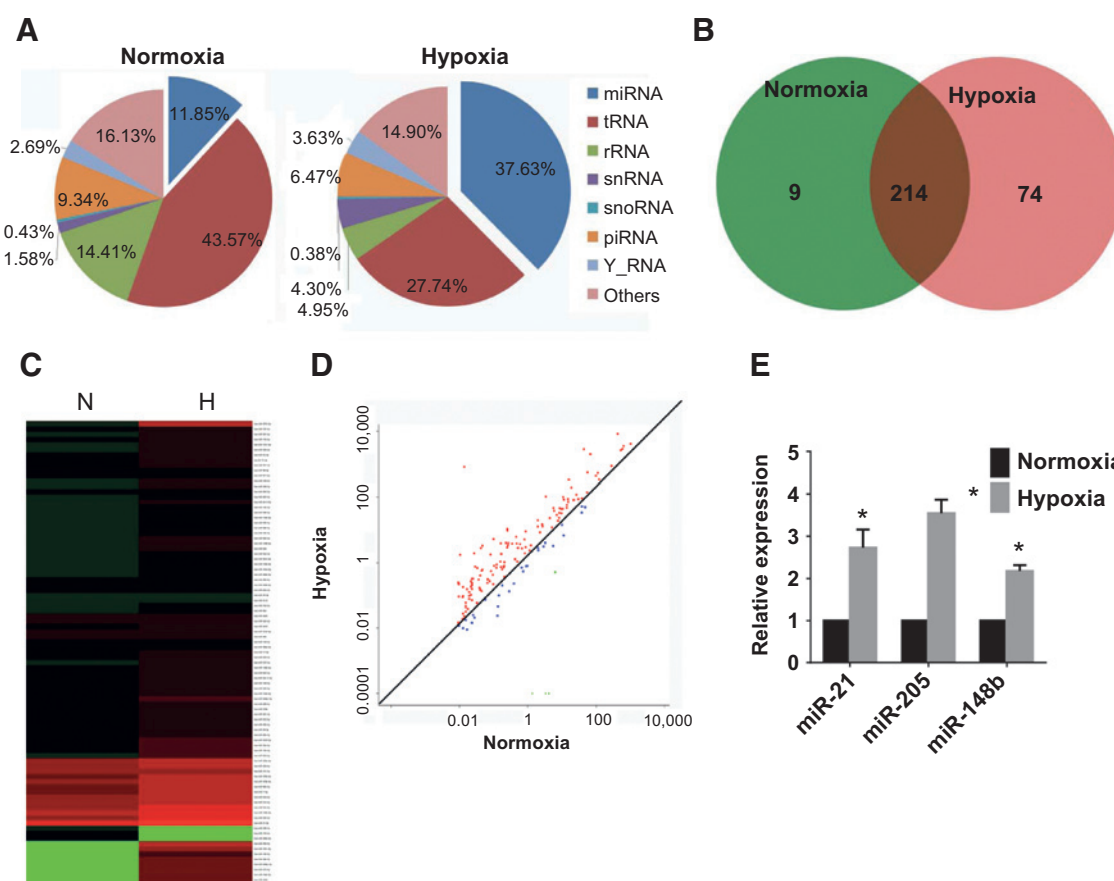


Figure 2. miRNA expression profiles of hypoxic tumor-derived exosomes. A, the percentage of small RNA categories in all reads mapped to noncoding RNA databases. B, Venn diagram showing the unique and overlapping miRNAs between normoxic and hypoxic exosomes. C, heatmap diagram of differential miRNA expression between normoxic and hypoxic exosomes. Gene expression data were obtained using next-generation sequencing on the Illumina HiSeq 2500 platform. Expression values shown are mean centered. Red, increased expression; green, decreased expression; and black, mean value. D, differentially expressed miRNAs between the normoxia and hypoxia groups. Red, increased expression; green, decreased expression; and blue, no difference. $P < 0.05$ and fold change > 2 were considered significant. E, quantitative real-time PCR validated the increase of miR-21, miR-205, and miR-148b in hypoxic exosomes. Experiments were performed in triplicate. *, $P < 0.01$.

threshold cutoff, we found that 108 miRNAs were significantly different between normoxic and hypoxic exosomes (Fig. 2C). Among the differentially expressed miRNAs, 105 miRNAs were upregulated in hypoxic exosomes compared with normoxic exosomes (Fig. 2D). To validate miRNA-seq results, exosomal levels of miR-21, miR-205, and miR-148b were measured by real-time PCR because these miRNAs present at high levels. Consistent with miRNA-seq, real-time PCR showed that exosomes derived from cells cultured under hypoxia had significantly increased miR-21, miR-205, and miR-148b levels compared with those derived from cells cultured under normoxic conditions (Fig. 2E).

Hypoxia stimulate exosomal miR-21 expression in HIF-1 α and HIF-2 α -dependent ways

We focused on miR-21 for further study because it was significantly increased in hypoxic exosomes and was expressed at the highest levels. To study whether hypoxia-induced miR-21 expression was HIF-1 α or HIF-2 α dependent, HIF-1 α and HIF-2 α were stably knocked down in Cal-27 cells by lentiviral shRNAs. In normoxic conditions, cellular and exosomal miR-21 levels were not significantly affected by either HIF-1 α or HIF-2 α knockdown

(Fig. 3A). In hypoxic conditions, however, both cellular and exosomal miR-21 levels were significantly decreased by HIF-1 α or HIF-2 α knockdown (Fig. 3B). These results were confirmed in an additional OSCC cell line SCC-9 (Supplementary Fig. S2), suggesting that hypoxia-induced cellular and exosomal miR-21 expression is dependent on both HIF-1 α and HIF-2 α in OSCC.

ChIP assays were used to further validate the binding of HIF-1 α and HIF-2 α to the predicted HRE region of miR-21. PCR products corresponding to the miR-21 HRE-containing promoter region were detected in cells cultured in 1% O₂ after HIF-1 α and HIF-2 α immunoprecipitation (Fig. 3C). The miR-130 promoter region, which does not contain an HRE, did not show any measurable recruitment of HIF-1 α or HIF-2 α under hypoxia. These results confirmed the direct binding of both HIF-1 α and HIF-2 α to the HRE region of miR-21 upon exposure to hypoxia.

miR-21 mediated hypoxic exosome-induced cell migration and invasion

To study the function of exosomal miR-21, we inhibited miR-21 in Cal-27 cells by lentiviral shRNA (30) and overexpressed miR-21 using the mimics. The knockdown of miR-21 resulted in a

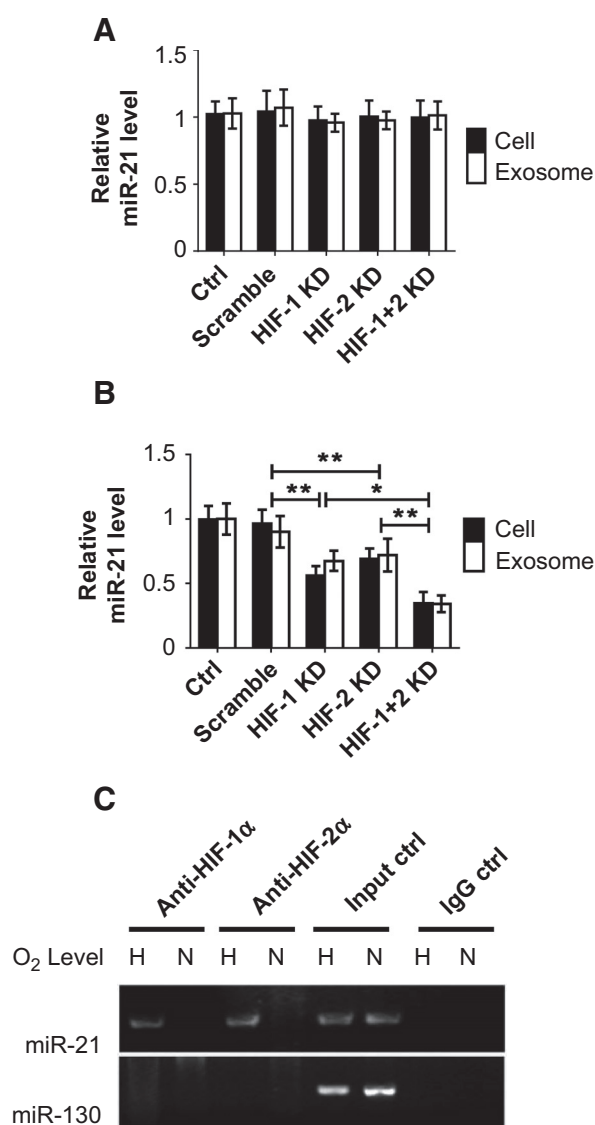


Figure 3. Hypoxia stimulates exosomal miR-21 expression in a HIF-1 α and HIF-2 α -dependent manner. miR-21 expression levels in exosomes and corresponding cells cultured under normoxia (A) and hypoxia (B) were measured by quantitative real-time PCR. Values represent the means \pm SD of triplicate experiments. Error bars, SD. *, $P < 0.05$. C, to detect binding of HIF-1 α and HIF-2 α to the miR-21 promoter, a ChIP assay was performed with the miR-21 promoter fragment containing the HRE. Input DNA that was not enriched by immunoprecipitation was amplified as a positive control. miR-130b (hypoxia nonresponsive) was used as a negative control.

76% decrease of miR-21 in tumor-derived exosomes (Supplementary Fig. S3A). The overexpression by miR-21 mimics resulted in a 3.21-fold and 2.73-fold increase of miR-21 in cells and exosomes, respectively, as determined by qRT-PCR (Supplementary Fig. S3B). Tumor cells were treated with normoxic and hypoxic exosomes derived from wild-type and miR-21 KD cells. As shown in Fig. 4A, the knockdown of miR-21 significantly decreased the migration of target cells compared with wild-type exosomes. We next investigated the roles of exosomal miR-21 on cell invasion. The invasion of cells treated with miR-21 KD

exosomes was significantly inhibited compared with that of cells treated with control exosomes (Fig. 4B).

To study whether hypoxic exosome-induced migration and invasion are dependent on miR-21, miR-21 was overexpressed in HIF-1 α and HIF-2 α KD cells. The expression of miR-21 mimics in HIF-1 α and HIF-2 α KD cells restored miR-21 levels in exosomes. Furthermore, the restoration of miR-21 levels in exosomes increased target cell migration (Fig. 4C) and invasion (Fig. 4D). The protein levels of validated targets of miR-21 were significantly downregulated by exosomal miR-21 in the treated cells (Supplementary Fig. S3C). Moreover, we examined whether exosomal miR-21 induced EMT-related changes in OSCC cells and found that exosomal miR-21 markedly enhanced vimentin expression while significantly decreasing E-cadherin levels in treated cells (Supplementary Fig. S3C). Exosomal miR-21 also induced the expression of snail, a key EMT regulatory factor (Supplementary Fig. S3C). These results suggest that hypoxic exosome-induced cell migration and invasion are dependent on miR-21, which downregulates a pool of target genes, and induces EMT of the target cells.

Tumor-derived exosomal miR-21 induced tumor growth and metastasis in a xenograft model

Because the hypoxic tumor-derived exosomes induced the migration and invasion of normoxic cells, we hypothesized that cells in the hypoxic region of a tumor may induce cells in the normoxic region to migrate and invade through the activity of exosomal miR-21. To investigate the role of tumor-derived exosomal miR-21 in tumor growth and metastasis, Cal-27 (1×10^6) cells were injected subcutaneously in nu/nu mice to generate tumors with a size of 60 mm³. Hypoxic and normoxic exosomes (10 μ g) were then injected into the center of the xenograft tumors. The overexpression of miR-21 in normoxic exosomes increased the growth and weight of the tumor. miR-21 KD abrogated the promotion of tumor growth by hypoxic exosomes (Fig. 5A).

Ten percent of mice treated with normoxic exosomes were positive for lymph node metastasis, whereas 40% and 50% of mice treated by hypoxic and miR-21-overexpressing exosomes, respectively, were positive for metastasis (Fig. 5B). The knockdown of miR-21 in hypoxic exosomes significantly inhibited the lymph node metastasis of xenograft tumors (Fig. 5B). No mouse in any group was positive for metastatic tumors in the lung.

We next investigated whether exosomal miR-21 regulates its target genes and EMT *in vivo*. Consistent with the *in vitro* experiments, hypoxic exosome- and miR-21-overexpressing exosome-treated tumors had decreased expression of validated miR-21 targets (Fig. 5C). Moreover, hypoxic exosomes and miR-21-overexpressing exosomes significantly induced the expression of vimentin, while markedly decreasing the expression of E-cadherin. The knockdown of miR-21 in hypoxic exosomes restored the expression of E-cadherin (Fig. 5C and D).

Circulating exosomal miR-21 levels were correlated with lymph node metastasis in OSCC patients

We isolated and characterized exosomes from the serum of patients with OSCC and paired healthy volunteers. There was no difference between patients and healthy volunteers, in age, gender, smoking, and alcohol status (Supplementary Table S3). Three tubes of blood samples were obtained from each patient or healthy volunteers. The purified exosomes showed a size distribution consistent with exosome vesicles (50–200 nm, Fig. 6A) as

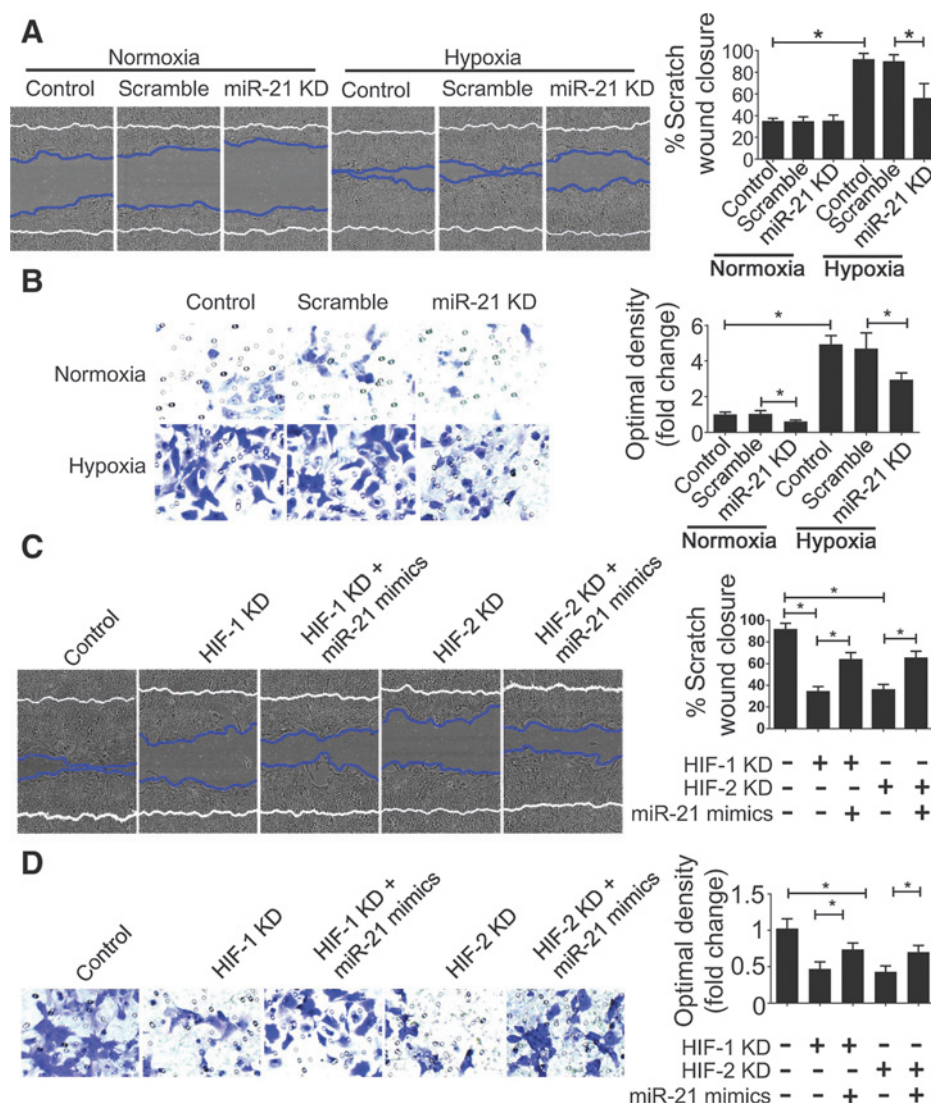


Figure 4. The role of miR-21 in the regulation of hypoxic exosome-induced migration and invasion. A and C, analysis of tumor cell migration by *in vitro* scratch assays. Images were acquired at 0 (white line) and 24 hours (blue line). Right, quantitative analysis of scratch wound closure. B and D, the invasiveness of exosome-treated OSCC cells was assessed using an invasion assay (magnification, $\times 200$). Data represent at least three experiments performed in triplicate. *, $P < 0.01$; **, $P < 0.001$.

measured by electron microscopy. Western blots showed that these exosomes were highly enriched for the exosome-associated proteins CD63 and CD81 compared with serum (Supplementary Fig. S3D). Total RNA was extracted from circulating exosomes. We compared the mean value of miR-21 between 3 different samples of each patient. No significant difference was observed between samples from 103 (95.4%) patients (data not shown), suggesting that the circulating exosomal miR-21 levels are reproducible. More importantly, patients with OSCC had significantly higher levels of circulating exosomal miR-21 compared with paired healthy volunteers (Fig. 6B).

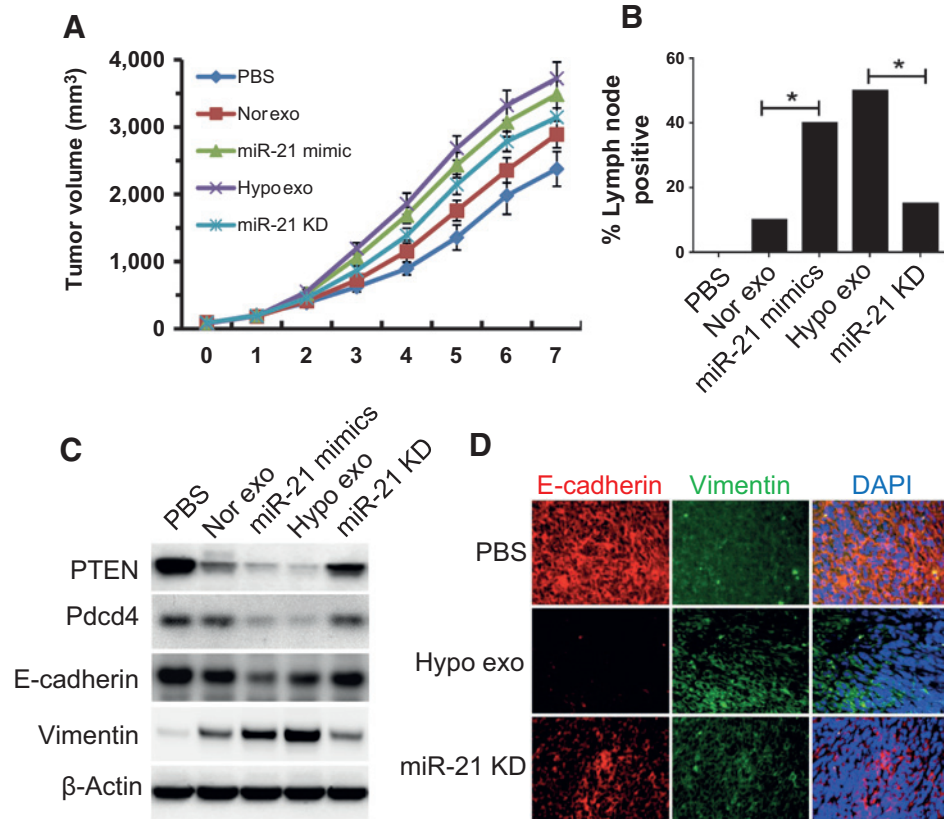
To analyze the correlation between exosomal miR-21 and clinical-pathologic parameters, the median miR-21 level was regarded as the cut-off point for low and high expression. Circulating exosomal miR-21 levels were closely associated with T stage ($P = 0.009$) and lymph node metastasis ($P = 0.021$) of patients with OSCC (Table 1). To further study the correlation between exosomal miR-21 and the hypoxic tumor microenvironment, HIF-1 α and HIF-2 α expression was measured by immunohistochemical staining. Nuclear staining of HIF-1 α and HIF-2 in cancer

cells was regarded as positive (Fig. 6C). Circulating exosomal miR-21 significantly correlated with both HIF-1 α and HIF-2 α staining. The analyses using mean miR-21 levels as the cut-off point confirmed the significant correlations between circulating exosomal miR-21 and T stage, lymph node metastasis, HIF-1 α expression, and HIF-2 α expression (data not shown). We then made comparisons of all individual levels of miR-21 rather than ranking them as low and high expression using Spearman correlation test. It was showed that circulating exosomal miR-21 was significantly correlated with T stage ($P = 0.023$), lymph node metastasis ($P = 0.008$), and HIF-1 α expression ($P = 0.006$). No significance was observed between miR-21 and HIF-2 α expression ($P = 0.053$), which is inconsistent with those analyses using the cutoffs.

To investigate whether the circulating exosomes are biologically active, we treated OSCC cell lines with circulating exosomes purified from 3 healthy volunteers and 3 patients respectively. Exosomes from healthy volunteers and patients significantly increased both migration (Supplementary Fig. S4A) and invasion (Supplementary Fig. S4B) of OSCC cells compared with PBS-treated controls. No significant difference was observed between

Figure 5.

The role of tumor-derived exosomal miR-21 in tumor growth and metastasis in a xenograft model. A, growth curve of xenograft tumors. *, $P < 0.05$. B, the percentage of mice with OSCC xenograft with lymph node involvement was treated with different exosomes as indicated. *, $P < 0.05$. C, protein levels of PTEN, Pcd4, E-cadherin, and vimentin were measured by Western blot analysis. β -Actin was used as the internal control. D, representative image of immunofluorescence staining shows the expression of E-cadherin and vimentin in xenograft tumors. Hypo exo, hypoxic exosome.



patients and healthy volunteers; although these patients had significantly increased exosomal miR-21 levels than healthy volunteers (Supplementary Fig. S4C). These results indicate that the circulating exosomes are biologically active and that there should be other factors, other than miR-21, that also contribute to the cell migration and invasion.

These data, along with the above *in vitro* and *in vivo* results, indicate that the hypoxic microenvironment may stimulate tumor

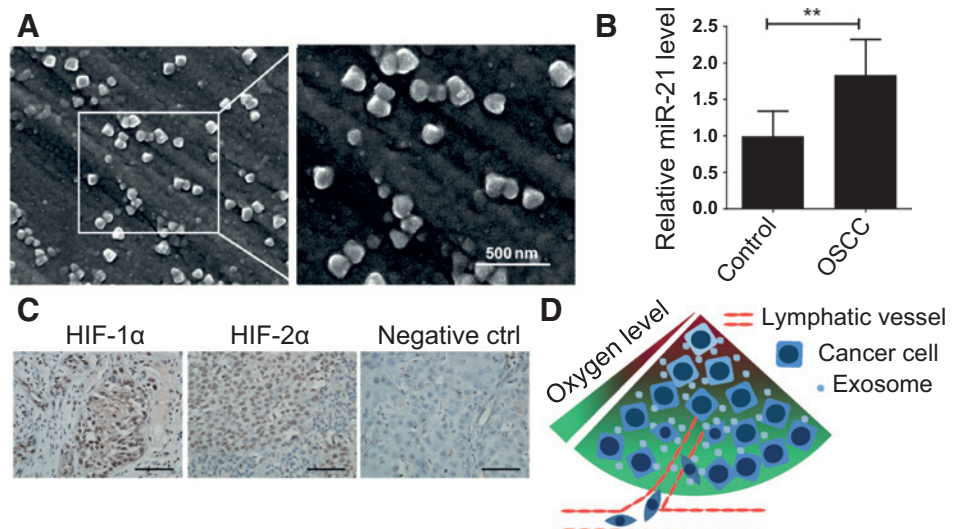
cells to produce exosomes that carry greater amounts of miR-21. These miR-21-rich exosomes would potentially then induce nonhypoxic cells to invade and metastasize (Fig. 4D).

Discussion

Exosomes were originally described in the 1980s, and recent studies have demonstrated that exosomes contain not only lipids

Figure 6.

Circulating exosomal miR-21 levels correlated with lymph node metastasis in OSCC patients. A, representative electron micrograph of exosomes isolated from the serum of patients with OSCC. Scale bar, 500 nm. B, exosomal miR-21 levels were measured by qRT-PCR. Values represent means \pm SD. Error bars, SD. *, $P < 0.05$. C, representative image of HIF-1 α and HIF-2 α expression in OSCC samples by immunohistochemical staining. (magnification, $\times 400$; scale bar, 50 μ m). D, schematic cartoon illustrating that hypoxic tumor-derived exosomes may transit to normoxic regions and drive nonhypoxic cells toward a prometastatic phenotype.



and proteins but also small RNAs, particularly miRNAs (11, 17–19). In this study, we initially purified exosomes from the supernatant of OSCC cells, and explored the miRNA expression profiles of exosomes derived from hypoxic and normoxic OSCC cells using miRNA-seq. We found that hypoxia increased tumor-derived exosomal miR-21 levels, which induced migration and invasion of target normoxic cells both *ex vivo* and *in vivo*. Finally, we demonstrated that circulating exosomal miR-21 was correlated with the hypoxic status of tumors and lymph node involvement in patients with OSCC. We therefore suggest that the hypoxic microenvironment may stimulate tumor cells to produce exosomes that carry increased amounts of miR-21. These miR-21-rich tumor-derived exosomes may be distributed to normoxic regions and drive nonhypoxic cells toward a prometastatic phenotype. This is the first study, to our knowledge, suggesting that exosomes function as a bridge between normoxic and hypoxic cancer cells in the tumor microenvironment by transferring miRNAs.

It has been well recognized that hypoxia is a powerful driving force for tumor progression by regulating pathways that are involved in tumor glycolysis, angiogenesis, immortalization, growth factor signaling, genetic instability, tissue invasion, and metastasis (5, 6). Recently, there has been a growing body of evidence showing that exosomes participate in tumor progression (21–25, 38). However, the cellular and molecular mechanisms underlying the association between exosomes and hypoxia in the regulation of cancer progression have not been well clarified. It has been reported that hypoxia promotes the release of exosomes by breast cancer cells (21). In addition, exosomes derived from hypoxic glioblastoma multiforme (26) and leukemia (28) cells may induce angiogenesis through the phenotypic modulation of endothelial cells. Recently, Aga and colleagues (39) demonstrated that exosome-mediated transfer of endogenous HIF-1 α by nasopharyngeal carcinoma cells to surrounding tumor cells promoted cancer progression. Here, we show that hypoxia induced the release of exosomes by OSCC cell lines and that exosomes derived from hypoxic OSCC cells promote tumor migration and invasion of recipient normoxic cells. Moreover, this hypoxic exosome-induced cell migration and invasion are dependent on miR-21, which downregulates its target genes and induces EMT of the recipient normoxic cells. Our results, along with previous reports, suggest that exosomes are important components of the tumor microenvironment and act as a messenger that transports signals between cells. By means of exosomes, tumor cells in the hypoxic region could render recipient cells in the normoxic region more invasive and aggressive.

Exosomes contain a wide contingent of functional proteins, mRNAs and miRNAs (17–19). Because the transfer of proteins between cells has been well established while the horizontal transfer of functional RNA molecules via exosomes has not been well clarified, we focused in this study on the function of exosomal miRNAs in tumor progression. Using next-generation sequencing, we identified miRNA expression profiles in OSCC-derived exosomes under both hypoxic and normoxic conditions. We identified 223 and 288 known miRNAs in normoxic and hypoxic exosomes, respectively. Among the identified known miRNAs, 74 miRNAs were uniquely expressed in hypoxic exosomes (Fig. 2B). However, 56 of 74 miRNAs are not significantly different between normoxic and hypoxic exosomes. The reason might be that these miRNAs are expressed in a very low level in the exosomes. The miRNA-seq revealed 108 miRNAs that were differentially expressed between normoxic and hypoxic exosomes, among

which 18 miRNAs were uniquely expressed in hypoxic exosomes and 90 miRNAs were overlapped in both conditions. This study is the first to compare the miRNA profiles between normoxic and hypoxic exosomes derived from OSCC cells. It has been suggested that some miRNAs may be uniquely packed into exosomes and that the exosomal miRNA profile does not reflect that of the donor cell (28, 40). However, it has also been reported that exosomal miRNA profiles resemble those of the parent cells (41). In this study, no cellular miRNA expression profile was determined for the comparison with the exosomal miRNA profile, which is a shortcoming of the work. Using miR-21 as an example, we showed that both cellular and exosomal miR-21 levels were significantly increased under hypoxia, suggesting that exosomal miRNA may at least partially reflect cellular miRNA profiles.

miR-21 shows features of oncomirs by targeting many tumor suppressor genes related to cell proliferation, apoptosis, and invasion in multiple histologic types of cancer, including OSCC (42, 43). Recently, studies have demonstrated that hypoxia induces miR-21 expression in a HIF-1 α -dependent manner in pancreatic cancer cells (44) and cardiomyocytes (36). In contrast, in renal cancer, it has been suggested that the dysregulation of miR-21 is HIF-independent (45). In this article, we showed that hypoxia enhanced miR-21 levels in both OSCC cells and OSCC-derived exosomes. This induction of miR-21 by hypoxia was directly regulated by both HIF-1 α and HIF-2 α in OSCC cells. Hence, we suggest that HIF-1 α and HIF-2 α play overlapping roles in the hypoxic induction of miR-21 in OSCC. Considering the variations among different types of tumors, there may be tissue-specific mechanisms of miR-21 regulation in response to hypoxia.

Our results showed that miR-21 had the highest levels among the differentially expressed miRNAs in normoxic and hypoxic exosomes. Although miR-21 has been demonstrated to be overexpressed in many types of cancer and to promote cancer cell proliferation, migration, and survival (43), the function of exosomal miR-21 in oral cancer progression is uncharacterized. We therefore further investigated the function of exosomal miR-21 in the hypoxic exosome-mediated modulation of cancer progression. We found that miR-21 KD in exosomes decreased the migration and invasion of recipient cells and that the restoration of miR-21 in HIF-1 α and HIF-2 α KD exosomes reestablished the migration and invasion of target cells both *ex vivo* and *in vivo*. We suggest that, when internalized by recipient cells, exosomes deliver exogenous miR-21 that downregulates a pool of genes and induces EMT of these cells. A recent study showed that transformed human bronchial epithelial cells release exosomes containing miR-21, which stimulated proliferation in neighboring normal cells (46). In addition, Fabbri and colleagues (47) demonstrated that lung cancer-secreted exosomal miR-21 binds as a ligand to the Toll-like receptor (TLR) family in immune cells, triggering a TLR-mediated prometastatic inflammatory response that ultimately may lead to tumor growth and metastasis. These results, along with ours, suggest that cancer cell-derived exosomal miR-21 is involved in tumor microenvironment interactions and is important for tumor growth and spread.

Given the important role of exosomal miR-21 in modulating the tumor microenvironment, we studied whether circulating exosomal miR-21 could serve as a valuable biomarker for the diagnosis and prognosis of OSCC. We found that patients with OSCC had significantly higher levels of circulating exosomal miR-21 and that the level of circulating exosomal miR-21 was associated with T stage and lymph node metastasis. Moreover,

circulating exosomal miR-21 correlated with tumor HIF α expression, reflecting the hypoxic status of cancer. Our results were consistent with previous reports showing that serum exosomal miR-21 correlated with advanced tumor stage in hepatocellular carcinoma (48), esophageal squamous cell carcinoma (49), and laryngeal squamous cell carcinoma (50). These results provide novel evidence that circulating exosomal miR-21 may serve as a potential biomarker for the diagnosis and prognosis of many types of cancer.

Although the differences are statistically significant, the HIF α knockdown had a moderate effect on miR-21 expression, and the effects of exosomal miR-21 on tumor growth are also modest. The reason is that there might be other factors, other than miR-21, are also playing major roles in these processes. Among the 108 differentially expressed miRNAs, we only focused on miR-21 that had the highest levels in the tumor-derived exosomes. Whether the rest 107 differentially expressed miRNAs could contribute to the exosome-induced cell migration and invasion needs to be investigated in the further studies. Moreover, the protein cargo of exosomes might also play important roles in the cancer progression, which are also needed to be explored in the future.

In this article, we provide evidence that hypoxia increases the miR-21 levels in tumor-derived exosomes. These miR-21-rich tumor-derived exosomes are internalized by normoxic cells and drive recipient cells toward a prometastatic phenotype. We there-

fore conclude that tumor-derived exosomes may function as a messenger that delivers miRNAs between normoxic and hypoxic cancer cells and thus remodels the tumor microenvironment of OSCC.

Disclosure of Potential Conflicts of Interest

No potential conflicts of interest were disclosed.

Authors' Contributions

Conception and design: G. Zhu

Development of methodology: L. Li, S. Wang, W. Wang, X. Li, K. Liu

Acquisition of data (provided animals, acquired and managed patients, provided facilities, etc.): S. Wang, J. Jiang, K. Liu, Chunhua Li

Analysis and interpretation of data (e.g., statistical analysis, biostatistics, computational analysis): Z. Wang, J. Jiang

Writing, review, and/or revision of the manuscript: G. Zhu

Administrative, technical, or material support (i.e., reporting or organizing data, constructing databases): Chao Li, Z. Wang, J. Chen

Grant Support

This work was supported by the National Natural Science Foundation of China (grant no. 81302375 and 81200771).

The costs of publication of this article were defrayed in part by the payment of page charges. This article must therefore be hereby marked *advertisement* in accordance with 18 U.S.C. Section 1734 solely to indicate this fact.

Received June 18, 2015; revised October 17, 2015; accepted November 9, 2015; published OnlineFirst March 18, 2016.

References

- Jemal A, Bray F, Center MM, Ferlay J, Ward E, Forman D. Global cancer statistics. *CA Cancer J Clin* 2011;61:69–90.
- Sano D, Myers JN. Metastasis of squamous cell carcinoma of the oral tongue. *Cancer Metastasis Rev* 2007;26:645–62.
- Kowalski LP, Sanabria A. Elective neck dissection in oral carcinoma: a critical review of the evidence. *Acta Otorhinolaryngol Ital* 2007;27:113–7.
- Neville BW, Day TA. Oral cancer and precancerous lesions. *CA Cancer J Clin* 2002;52:195–215.
- Lu X, Kang Y. Hypoxia and hypoxia-inducible factors: master regulators of metastasis. *Clin Cancer Res* 2010;16:5928–35.
- Harris AL. Hypoxia—a key regulatory factor in tumour growth. *Nat Rev Cancer* 2002;2:38–47.
- Brahimi-Horn MC, Chiche J, Pouyssegur J. Hypoxia and cancer. *J Mol Med* 2007;85:1301–7.
- Lofstedt T, Fredlund E, Holmquist-Mengelbier L, Pietras A, Ovenberger M, Poellinger L, et al. Hypoxia inducible factor-2 α in cancer. *Cell Cycle* 2007;6:919–26.
- Semenza GL. Defining the role of hypoxia-inducible factor 1 in cancer biology and therapeutics. *Oncogene* 2010;29:625–34.
- Zhu GQ, Tang YL, Li L, Zheng M, Jiang J, Li XY, et al. Hypoxia inducible factor 1 α and hypoxia inducible factor 2 α play distinct and functionally overlapping roles in oral squamous cell carcinoma. *Clin Cancer Res* 2010;16:4732–41.
- van Niel G, Porto-Carreiro I, Simoes S, Raposo G. Exosomes: a common pathway for a specialized function. *J Biochem* 2006;140:13–21.
- Thery C, Zitvogel L, Amigorena S. Exosomes: composition, biogenesis and function. *Nat Rev Immunol* 2002;2:569–79.
- Schorey JS, Bhatnagar S. Exosome function: from tumor immunology to pathogen biology. *Traffic* 2008;9:871–81.
- Wahlgren J, De LKT, Brisslet M, Vaziri Sani F, Teleme E, Sunnerhagen P, et al. Plasma exosomes can deliver exogenous short interfering RNA to monocytes and lymphocytes. *Nucleic Acids Res* 2012;40:e130.
- Peinado H, Lavotshkin S, Lyden D. The secreted factors responsible for pre-metastatic niche formation: old sayings and new thoughts. *Semin Cancer Biol* 2011;21:139–46.
- O'Loughlin AJ, Woffindale CA, Wood MJ. Exosomes and the emerging field of exosome-based gene therapy. *Curr Gene Ther* 2012;12:262–74.
- Mathivanan S, Ji H, Simpson RJ. Exosomes: extracellular organelles important in intercellular communication. *J Proteomics* 2010;73:1907–20.
- Valadi H, Ekstrom K, Bossios A, Sjostrand M, Lee JJ, Lotvall JO. Exosome-mediated transfer of mRNAs and microRNAs is a novel mechanism of genetic exchange between cells. *Nat Cell Biol* 2007;9:654–9.
- Skog J, Wurdinger T, van Rijn S, Meijer DH, Gainche L, Sena-Estevés M, et al. Glioblastoma microvesicles transport RNA and proteins that promote tumour growth and provide diagnostic biomarkers. *Nat Cell Biol* 2008;10:1470–6.
- Martins VR, Dias MS, Hainaut P. Tumor-cell-derived microvesicles as carriers of molecular information in cancer. *Curr Opin Oncol* 2013;25:66–75.
- King HW, Michael MZ, Gleadle JM. Hypoxic enhancement of exosome release by breast cancer cells. *BMC Cancer* 2012;12:421.
- Webber J, Steadman R, Mason MD, Tabi Z, Clayton A. Cancer exosomes trigger fibroblast to myofibroblast differentiation. *Cancer Res* 2010;70:9621–30.
- Liu C, Yu S, Zinn K, Wang J, Zhang L, Jia Y, et al. Murine mammary carcinoma exosomes promote tumor growth by suppression of NK cell function. *J Immunol (Baltimore, Md: 1950)* 2006;176:1375–85.
- Hood JL, San RS, Wickline SA. Exosomes released by melanoma cells prepare sentinel lymph nodes for tumor metastasis. *Cancer Res* 2011;71:3792–801.
- Peinado H, Aleckovic M, Lavotshkin S, Matei I, Costa-Silva B, Moreno-Bueno G, et al. Melanoma exosomes educate bone marrow progenitor cells toward a pro-metastatic phenotype through MET. *Nat Med* 2012;18:883–91.
- Kucharzewska P, Christianson HC, Welch JE, Svensson KJ, Fredlund E, Ringner M, et al. Exosomes reflect the hypoxic status of glioma cells and mediate hypoxia-dependent activation of vascular cells during tumor development. *Proc Natl Acad Sci U S A* 2013;110:7312–7.
- Park JE, Tan HS, Datta A, Lai RC, Zhang H, Meng W, et al. Hypoxic tumor cell modulates its microenvironment to enhance angiogenic and metastatic potential by secretion of proteins and exosomes. *Mol Cell Proteomics* 2010;9:1085–99.
- Tadokoro H, Umezaki T, Ohyashiki K, Hirano T, Ohyashiki JH. Exosomes derived from hypoxic leukemia cells enhance tube formation in endothelial cells. *J Biol Chem* 2013;288:34343–51.

29. Zhu G, Tang Y, Geng N, Zheng M, Jiang J, Li L, et al. HIF- α /MIF and NF- κ B/IL-6 axes contribute to the recruitment of CD11b+Gr-1+ myeloid cells in hypoxic microenvironment of HNSCC. *Neoplasia* 2014;16:168–79.
30. Yang CH, Yue J, Pfeffer SR, Handorf CR, Pfeffer LM. MicroRNA miR-21 regulates the metastatic behavior of B16 melanoma cells. *J Biol Chem* 2011;286:39172–8.
31. Yang C, Kim SH, Bianco NR, Robbins PD. Tumor-derived exosomes confer antigen-specific immunosuppression in a murine delayed-type hypersensitivity model. *PLoS One* 2011;6:e22517.
32. Singh R, Pochampally R, Watabe K, Lu Z, Mo YY. Exosome-mediated transfer of miR-10b promotes cell invasion in breast cancer. *Mol Cancer* 2014;13:256.
33. Kroh EM, Parkin RK, Mitchell PS, Tewari M. Analysis of circulating microRNA biomarkers in plasma and serum using quantitative reverse transcription-PCR (qRT-PCR). *Methods* 2010;50:298–301.
34. Holmquist-Mengelbier L, Fredlund E, Lofstedt T, Noguera R, Navarro S, Nilsson H, et al. Recruitment of HIF-1 α and HIF-2 α to common target genes is differentially regulated in neuroblastoma: HIF-2 α promotes an aggressive phenotype. *Cancer Cell* 2006;10:413–23.
35. Liang CC, Park AY, Guan JL. *In vitro* scratch assay: a convenient and inexpensive method for analysis of cell migration *in vitro*. *Nat Protoc* 2007;2:329–33.
36. Liu Y, Nie H, Zhang K, Ma D, Yang G, Zheng Z, et al. A feedback regulatory loop between HIF-1 α and miR-21 in response to hypoxia in cardiomyocytes. *FEBS Lett* 2014;588:3137–46.
37. Kulshreshtha R, Ferracin M, Wojcik SE, Garzon R, Alder H, Agosto-Perez FJ, et al. A microRNA signature of hypoxia. *Mol Cell Biol* 2007;27:1859–67.
38. Luga V, Zhang L, Vitoria-Petit AM, Ogunjimi AA, Inanlou MR, Chiu E, et al. Exosomes mediate stromal mobilization of autocrine Wnt-PCP signaling in breast cancer cell migration. *Cell* 2012;151:1542–56.
39. Aga M, Bentz GL, Raffa S, Torrisi MR, Kondo S, Wakisaka N, et al. Exosomal HIF1 α supports invasive potential of nasopharyngeal carcinoma-associated LMP1-positive exosomes. *Oncogene* 2014;33:4613–22.
40. Rana S, Malinowska K, Zoller M. Exosomal tumor microRNA modulates premetastatic organ cells. *Neoplasia* 2013;15:281–95.
41. Liao J, Liu R, Yin L, Pu Y. Expression profiling of exosomal miRNAs derived from human esophageal cancer cells by Solexa high-throughput sequencing. *Int J Mol Sci* 2014;15:15530–51.
42. Li J, Huang H, Sun L, Yang M, Pan C, Chen W, et al. MiR-21 indicates poor prognosis in tongue squamous cell carcinomas as an apoptosis inhibitor. *Clin Cancer Res* 2009;15:3998–4008.
43. Ng R, Song C, Roll GR, Frandsen NM, Willenbring H. A microRNA-21 surge facilitates rapid cyclin D1 translation and cell cycle progression in mouse liver regeneration. *J Clin Invest* 2012;122:1097–108.
44. Mace TA, Collins AL, Wojcik SE, Croce CM, Lesinski GB, Bloomston M. Hypoxia induces the overexpression of microRNA-21 in pancreatic cancer cells. *J Surg Res* 2013;184:855–60.
45. Neal CS, Michael MZ, Rawlings LH, Van der Hoek MB, Gleadle JM. The VHL-dependent regulation of microRNAs in renal cancer. *BMC Med* 2010;8:64.
46. Xu Y, Luo F, Liu Y, Shi L, Lu X, Xu W, et al. Exosomal miR-21 derived from arsenite-transformed human bronchial epithelial cells promotes cell proliferation associated with arsenite carcinogenesis. *Archives Toxicol* 2015;89:1071–82.
47. Fabbri M, Paone A, Calore F, Galli R, Gaudio E, Santhanam R, et al. MicroRNAs bind to Toll-like receptors to induce prometastatic inflammatory response. *Proc Natl Acad Sci U S A* 2012;109:E2110–6.
48. Wang H, Hou L, Li A, Duan Y, Gao H, Song X. Expression of serum exosomal microRNA-21 in human hepatocellular carcinoma. *BioMed Res Int* 2014;2014:864894.
49. Tanaka Y, Kamohara H, Kinoshita K, Kurashige J, Ishimoto T, Iwatsuki M, et al. Clinical impact of serum exosomal microRNA-21 as a clinical biomarker in human esophageal squamous cell carcinoma. *Cancer* 2013;119:1159–67.
50. Wang J, Zhou Y, Lu J, Sun Y, Xiao H, Liu M, et al. Combined detection of serum exosomal miR-21 and HOTAIR as diagnostic and prognostic biomarkers for laryngeal squamous cell carcinoma. *Med Oncol* 2014;31:148.